

# Exact Solutions for Certain Weighted Sum-rate and Common-rate Maximization Problems

by

Koosha Pourtahmasi Roshandeh

A thesis submitted in partial fulfillment of the requirements for the degree of

Master of Science

in

Communications

Department of Electrical and Computer Engineering

University of Alberta

© Koosha Pourtahmasi Roshandeh, 2017

# Abstract

Weighted sum-rate and common-rate optimization problems in wireless networks can be represented as the general forms of  $\max \sum_{i=1}^N a_i \log_2(1 + \gamma_i)$  and  $\max \min_i(\gamma_i)$ , respectively, where  $\gamma_i$  represents the signal to noise ratio (SNR) of user  $i$  and  $a_i$  is a constant weight. In general, these problems are hard to solve. In this thesis, we propose a framework for finding the optimal solution of a class of such problems. To develop this framework, we first pose the optimization problems in general forms. Subject to some conditions on the region of feasible SNRs, the optimal solutions then are analytically derived. We show that these solutions apply to several practical scenarios. In particular, we optimize two different two-way relay networks where either the relay has a large number of antennas or the users. For these systems, we derive closed-form expressions for the optimal weighted sum rate and common rate. Numerical results and simulations verify the optimality of the analytical approach.

# Acknowledgements

I want to thank my supervisors professors Masoud Ardakani and Chintha Tellambura who shed some light on the road of my research with their advice and ideas during my masters study at the University of Alberta. Moreover, I would like to thank professors Khabbazian and Liang for their valuable comments for improving the quality of the thesis. Furthermore, I would like to thank my friends who gave me all forms of assistance during my study at the University of Alberta. Last but not least, I want to thank my family—Heybat, Sima, Pooya and Hana— for their invaluable supports during the tough times. I am always in your debt.

# Contents

<b>1</b>	<b>Motivation</b>	<b>1</b>
1.1	Thesis Contributions . . . . .	3
1.2	Thesis Outline . . . . .	3
<b>2</b>	<b>Background</b>	<b>5</b>
2.1	Relaying . . . . .	5
2.2	Data Transmission Modes . . . . .	8
2.3	Receiver & Transmitter Diversity . . . . .	9
2.4	Jensen's inequality . . . . .	12
2.5	Arithmetic Mean-Geometric Mean Inequality . . . . .	14
2.6	Discrete memoryless channel, Capacity and Rate . . . . .	15
<b>3</b>	<b>A General Solution For a Class of WSR and CR Maximization</b>	<b>18</b>
3.1	Problem Definition . . . . .	18
3.2	Definitions and The Proposed Solutions . . . . .	19
3.2.1	Definitions . . . . .	19
3.2.2	The Proposed Solutions . . . . .	20
3.3	Two Mathematical Examples . . . . .	22
<b>4</b>	<b>Applications</b>	<b>24</b>
4.1	Two-way Relay Network with Single-antenna Relay . . . . .	24
4.1.1	System model . . . . .	24
4.1.2	Problem Formulation . . . . .	26

4.1.3	Optimal Power Allocation . . . . .	26
4.1.4	Ergodic sum rate . . . . .	28
4.1.5	Additional QoS constraints . . . . .	29
4.1.6	Numerical And Simulation Results . . . . .	33
4.2	Two-way Relay Network with Multiple-antenna Relay . . . . .	36
4.2.1	System model . . . . .	36
4.2.2	Common-rate . . . . .	38
4.2.3	Weighted sum-rate . . . . .	39
4.2.4	Numerical And Simulation Results . . . . .	40
4.3	Case Study: [ShahbazPanahi et al., 2012] . . . . .	41
<b>5</b>	<b>Conclusion &amp; Future Works</b>	<b>43</b>

# List of Figures

2.1	An example of relay communication. . . . .	5
2.2	Non-cooperative relaying. . . . .	7
2.3	Cooperative relaying. . . . .	7
2.4	Simplex Communication. . . . .	8
2.5	Half duplex Communication. . . . .	9
2.6	Full duplex Communication. . . . .	9
2.7	SISO system model. . . . .	10
2.8	MISO system model. . . . .	11
2.9	SIMO system model. . . . .	11
2.10	MIMO system model. . . . .	12
2.11	Discrete channel. . . . .	15
4.1	System model of a two-way relay network using multiple antennas. . . . .	25
4.2	Achievable sum rate performance using PPA and UPA with $\nu = 100$ , $\sigma_a^2 = \sigma_b^2 = 1$ , $m_b = 1$ and $N_0 = 1$ . . . . .	32
4.3	Achievable sum rate performance using PPA and UPA with $\nu = 20$ , $\sigma_a^2 = \sigma_b^2 = 1$ and $m_b = 1$ . . . . .	33
4.4	Impact of $\nu$ on the achievable sum rate with $\sigma_a^2 = \sigma_b^2 = 1$ , $m_b = 1$ , $N_0 = 1$ and $N_b = 1$ . . . . .	34
4.5	The achievable sum rate of Sub-Optimal PA for a feasible system with $\sigma_a^2 = \sigma_b^2 = 1, m_b = 1, N_0 = 1, N_b = 10, \zeta = 1.4$ and $\nu = 100$ . . . . .	34

4.6	The achievable sum rate of Sub-Optimal PA for an infeasible system with $\sigma_a^2 = \sigma_b^2 = 1$ , $m_b = 1$ , $N_0 = 1$ , $N_b = 10$ , $\zeta = 1.4$ and $\nu = 100$ . . . . .	35
4.7	The system model of a two-way relay network using multiple-antenna relay. . . . .	36
4.8	Achievable common-rate $a_1 = 2, a_2 = 1, \sigma_1^2 = 0.25, \sigma_2^2 = 1$ and $\sigma^2 = 1$ . . . . .	41
4.9	Achievable weighted sum-rate $a_1 = 2, a_2 = 1, \sigma_1^2 = 0.25, \sigma_2^2 = 1$ and $\sigma^2 = 1$ . . . . .	42

# List of Abbreviations

List of commonly used abbreviations

WSR	Weighted Sum Rate
CR	Common Rate
QoS	Quality of Service
MIMO	Multiple-Input Multiple-Output
AF	Amplify-and-Forward
DF	Decode-and-Forward
CF	Compress-and-Forward
SISO	Single Input-Single Output
MISO	Multiple Input- Single Output
SIMO	Single Input- Multiple Output
dB	Decibels
AWGN	Additive White Gaussian Noise
AM-GM	Arithmetic Mean-Geometric Mean
PA	Power Allocation
UPA	Uniform Power Allocation
SNR	Signal-to-Noise Ratio

# List of Symbols

## List of Symbols

$P_s$	Signal power
$P_n$	Noise power
$\Theta$	Feasible region of achievable SNRs
$\bar{\gamma}$	Vector of communication links SNRs
$\gamma_i$	SNR of $i$ -th communication link
$a_i$	Weight of $i$ -th communication link
$N_a$	Number of source $a$ antennas
$N_b$	Number of source $b$ antennas
$P_a$	Transmit power at the source $a$
$P_b$	Transmit power at the source $b$
$P_r$	Transmit power at the source $R$
$\mathbf{h}_a$	Channel coefficient between source $a$ and relay
$\mathbf{h}_b$	Channel coefficient between source $b$ and relay
$\mathbf{w}_l$	Transmit weight vector for source $l$
$G$	Relay gain
$\mathbf{n}_l$	Noise at source $l$
$m_l$	Fading parameter for source $l$
$\sigma_l$	Noise power at source $l$
$\bar{\mathbf{R}}$	Average sum rate

# Chapter 1

## Motivation

Wireless networks are inseparable parts of today's world. Various types of wireless networks such as wireless personal area networks (PANs), wireless local area networks (LANs), wireless ad hoc networks and cellular networks are widely used for different purposes. Satellites communication, medical applications and mobile communications are only a few examples of wireless network applications. The main advantages of wireless networks include enabling mobility, supporting numerous devices simultaneously and increasing efficiency in terms of cost and energy. Due to the success of wireless networks, the number of wireless devices has exploded and is predicted to exceed 40 billions by 2020 [1]. This has led to an emerging technology called 5G which will be the next generation of wireless technology providing faster speed, higher capacity and lower latency.

Wireless networks are evaluated based on various performance measures, e.g. throughput, spectral efficiency, power consumption and coverage. Hence, many efforts have been dedicated to improve their performance [2–12]. As a result, relays as a way of enhancing wireless networks performance have been introduced. Relays can help reduce the detrimental effects of path loss and shadowing in addition to increasing the path diversity in wireless networks [13]. Relays also enable wireless networks to achieve higher throughput and

spectral efficiency [13].

For wireless relay networks, weighted sum rate (WSR) and common rate (CR) maximizations are of great importance. The WSR and CR parameters are generally used for wireless resource management, cross-layer and beamforming design, link-scheduling, quality of service (QoS) and many more. For example, maximizing WSR in a multiple-input multiple-output (MIMO) system is equivalent to achieving a point on the boundary of the capacity region of the considered network [14]. The weight dedicated to a user of WSR maximization problem in a wireless network can be interpreted as the quality of service (QoS) provided by the service provider to that user. In a cognitive radio network, WSR maximization problem can be used for the optimal beamformer design [15]. Many power allocation strategies rely on WSR maximization problems in multi-way relay networks [16]. Furthermore, solving CR maximization problems is a way to follow fairness in wireless networks.

Despite the extensive applications of WSR and CR problems, the general WSR and CR maximizations are still open problems. For instance, the authors in [17] have shown that the general WSR problem is non-convex and NP-hard. To this end, many efforts have been dedicated to solve these problems under various assumptions and setups during past years.

Two general approaches have been used by researchers to attack WSR and CR maximizations. The first way is to convexify the problem in order to take advantage for standard convex optimization methods, e.g. Lagrange multipliers, Karush-Kuhn-Tucker conditions. Another approach is to employ numerical algorithms to solve these problems. Subgradient projection, Bundle, Cutting-plane and Dual subgradients and the drift-plus-penalty methods are some commonly used iterative algorithms. That said, in many cases even for fully convex cases, an analytical approach or a closed-form solution is not available. To this end, proposing a framework that offers an analytical approach or a closed-form solution in many cases for WSR or CR maximization problems

is of great interest.

## 1.1 Thesis Contributions

In this thesis, we propose a general framework for solving a class of optimization problems including WSR and CR optimization problems. To show the practicality and usefulness of the proposed framework, we also present a few examples which can be solved using the proposed framework. More specifically,

- We propose a theorem for solving a class of WSR maximization problems in wireless network based on Arithmetic mean-Geometric mean inequality.
- We present another theorem for solving CR optimization problems subject to satisfying a common feasibility constraint in wireless systems.
- For WSR maximization problem, we propose two novel practical examples of massive MIMO two-way relay networks. More specifically, we propose the optimal power allocations for solving WSR problems in different scenarios. Owing to the closed-form solution obtained using the proposed theorems for the first example, we also derive a closed-form expression for ergodic sum-rate of the users.
- We solve a new CR maximization problem using the proposed theorems. We also present the simulation results to verify our analysis.

## 1.2 Thesis Outline

This thesis is organized as follows. In Chapter 2, we discuss some essential concepts and background. Chapter 3 is divided into different sections as follows. Section 3.1 mathematically defines the problems of interest. In Section 3.2, using Arithmetic mean-Geometric mean inequality, we propose our main

theorems for solving the presented problems. Section 3.3, gives two simple mathematical examples for better illustration of the theorems. Chapter 4 provides some applications of the proposed theorems. More specifically, we propose two new examples of massive MIMO <sup>1</sup> two-way relay networks in Sections 4.1 and 4.2 to show the practicality of the presented theorems. In Section 4.3, we show that the results of [18] can be restated under the proposed theorems and can be solved using these theorems. In Chapter 5, some possible extensions of this work have been discussed. We also conclude our work in this chapter.

---

<sup>1</sup>Multiple Input-Multiple Output

# Chapter 2

## Background

### 2.1 Relaying

Relaying is a powerful communication method to improve the spectral efficiency of wireless networks [13]. This method is used when there is no direct link between the source and destination nodes or the received signal by the destination is weak (in terms of power, signal-to-noise ratio, etc.). Hence, the destination node is beyond the transmission range—the maximum distance that a node can send its data—of the source node. Figure 2.1 shows a wireless relay network.



Figure 2.1: An example of relay communication.

In a relaying protocol, the source node sends its information to the relay in the first time slot. The relay processes the received information and forwards it to the destination node in the second time slot. Based on the process that the relay performs on the received information, the relaying protocols are divided into three major categories: Amplify-and-Forward (AF), Decode-and-Forward

(DF) and Compress-and-Forward (CF) relaying. Different relaying protocols are explained in details below.

**Amplify and Forward Relaying:** Amplify and Forward (AF) relaying was first introduced in [19]. In this protocol, sender transmits its data to the relay in the first time slot and the relay amplifies the received signal with a factor and forwards it to the receiver in the second time slot. As we can see, information transmission is completed in two time slots. The major disadvantage of this strategy is that the noise will be magnified with the signal as the relay amplifies its received signal. However, the simplicity of this protocol made it very practical.

**Decode and Forward Relaying:** In this protocol, the sender sends its information to the relay in the first time slot. Then, the relay extracts the true signal from the received signal and decodes it. If the received signal can be decoded successfully, the relay forwards it to the receiver in the second time slot. However, the communication terminated when an error occurs during the decoding. As it can be seen, DAF strategy eliminates the noise in the received signal by the relay. However, privacy, complexity and delay are still major concerns of this strategy as the signal is being decoded by the relay.

**Compress and Forward Relaying:** The decoding part in this protocol is replaced with compression. That is, the received signal by the relay is compressed (instead of decoding) and is forwarded to the receiver. Various compression schemes can be used by the relay such as WynerZiv [20]. Discussing and comparing different compression schemes are avoided here since they are beyond the focus of this thesis.

Relaying schemes are divided into two categories based on the way the receiver is able to decode the true signal. This two categories is discussed below.

**Non-cooperative Relaying:** In this scheme, the receiver only uses the forwarded signal by the relay to decode the information of the sender. This

happens when there is no direct link between the sender and receiver and the sender signal cannot reach the receiver. Figure 2.2 illustrates non-cooperative relaying.

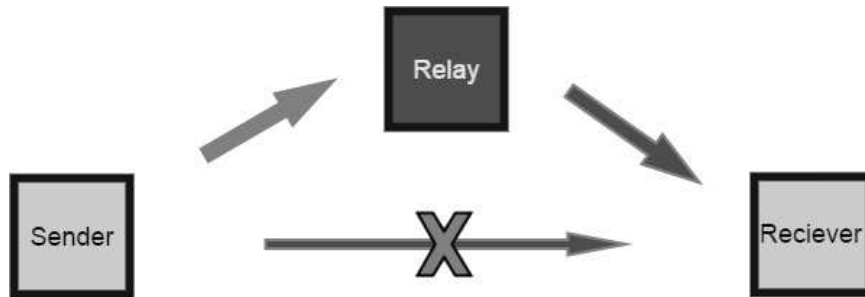


Figure 2.2: Non-cooperative relaying.

**Cooperative relaying:** In this protocol, there is a direct link between sender and receiver, and thus the received signal (sent by the sender) is available, but probably too weak to be decoded on its own. . In this case, the receiver combines the received signal of the sender and the forwarded signal of the relay to detect the true information. The major advantage of this scheme compared to the non-cooperative relaying scheme is the diversity gain which increases signal to noise ratio. Increasing the diversity gain significantly improves the chance of successful detection in wireless networks. Figure 2.3 shows this type of relaying.

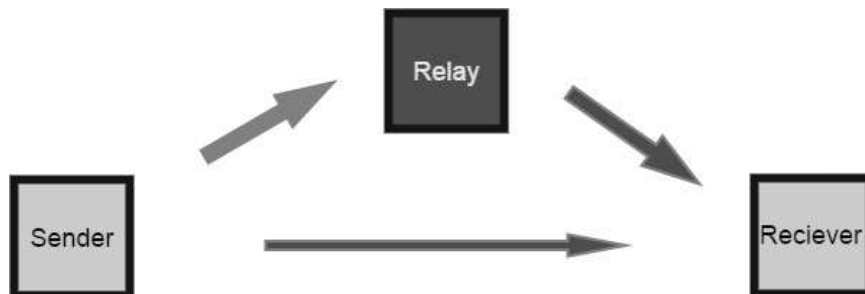


Figure 2.3: Cooperative relaying.

## 2.2 Data Transmission Modes

Data transmission between two wireless devices can occur in different modes. The difference between these modes are the direction of data transmission and/or the ability of a device to send and receive information simultaneously. We briefly discuss each mode below.

**Simplex:** In a simplex communication, information transmission occurs only in one direction. That means sender sends information to the receiver and the receiver can not reply. Some examples include satellite Internet connection, television broadcasting, the connection between a keyboard and the computer which employ simplex protocol for their communication. A simplex communication has been illustrated in Figure 2.4.

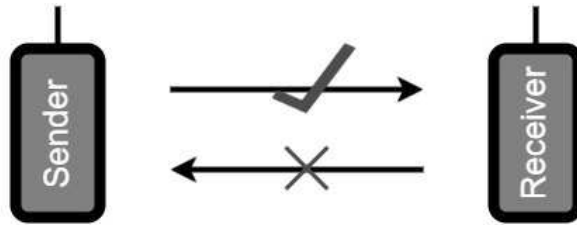


Figure 2.4: Simplex Communication.

**Half Duplex:** In a half duplex transmission mode, a device can send or receive information one at a time. In other words, the device cannot send and receive information simultaneously. However, information can be exchanged in both directions. Figure 2.5 illustrates a half duplex communication protocol.

Walkie-talkie is an example of half duplex protocol in which only one user can talk at a time and the other user should remain silent until the end of the first user's transmission.

**Full Duplex:** A user can simultaneously send and receive information in a full duplex communication protocol. A full duplex communication has been depicted in Figure 2.6. The major advantage of a full duplex protocol is speed. A full duplex communication system is much faster than a half duplex system

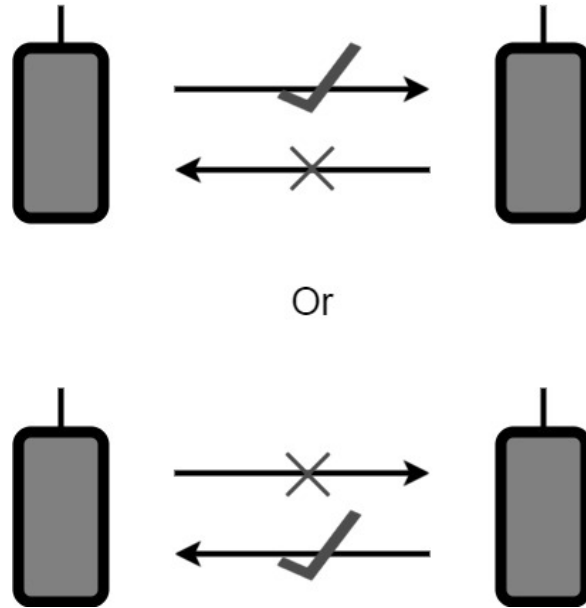


Figure 2.5: Half duplex Communication.

since the users do not need to stay silent while receiving information and are able to send and receive information simultaneously.

Telephones, modern I/O such as USB and computers connected via ethernet cable are some examples of full duplex devices. These devices are capable of sending and receiving data simultaneously.

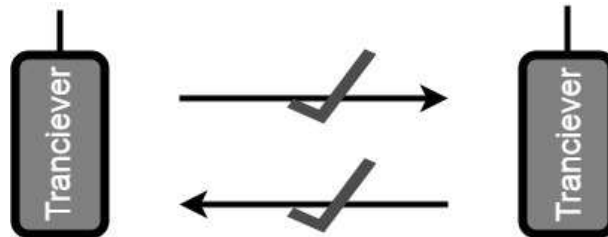


Figure 2.6: Full duplex Communication.

## 2.3 Receiver & Transmitter Diversity

A two-way communication system consists of a transmitter (source) and a receiver (destination). According to the number of antennas employed at

the source and destination, communication systems are divided into different groups: SISO (single input-single output), MISO (multiple input- single output), SIMO (single input- multiple output), MIMO (multiple input-multiple output) and massive MIMO. In this terminology, the word input refers to the transmitter as it sends the signal to the communication channel. Similarly, the word output refers to the receiver as it receives the output signal of the communication channel. Employing more than one antenna in a receiver or transmitter increases the data throughput (assuming a fixed bandwidth). However, increasing the number of antennas increases the complexity. In the following, each of the above five concepts is explained.

**SISO:** In this setup, the transmitter and receiver both use a single antenna for information transmission. Figure 2.7 shows a SISO system. The major advantage of these systems are their simplicity since they do not use any diversity technique. That is, the receiver does not need any further processing to employ diversity when it receives the signal. In this context, diversity refers to when a system uses two or more antennas to solve the problem of fading and interference by receiving different forms of a transmitted signal.

In SISO systems, interference and fading can reduce the SNR which can further results in lower data rate and capacity.



Figure 2.7: SISO system model.

**MISO:** Here, the transmitter uses multiple antennas and the receiver has single antenna. Transmit diversity is another term for this setup as it employs multiple antennas at the transmitter. A MISO system is depicted in Figure 2.8.

This model is used in communication between cell phones and base stations where the base stations use multiple antennas and each cell phone has a single antenna.

Using a single antenna at the receiver allows the receiver to be small. This also allows the receiver to be energy efficient and cost-effective.



Figure 2.8: MISO system model.

**SIMO:** In this setup, the transmitter has single antenna and the receiver has multiple antennas. This is also called receive diversity. Figure 2.9 illustrates this model. Opposite to MISO systems, employing multiple antennas at the receiver increases cost, energy consumption and size of the receiver device which can cause problems in some applications, e.g. mobile receivers.



Figure 2.9: SIMO system model.

**MIMO:** In MIMO systems, both transmitter and receiver have multiple antennas. A MIMO system has been depicted in Figure 2.10. Although employing multiple antennas at both receiver and transmitter adds some complexity to the system but it also increases the SNR of the received signal and therefore the communication capacity to a great extent [21]. Moreover, MIMO systems

benefit from multipath phenomenon <sup>1</sup> to increase the coverage range of signal transmission.

MIMO systems are widely used in different setups such as IEEE 802.11n, 4G, LTE-A, WiFi and WiMAX systems.



Figure 2.10: MIMO system model.

**Massive MIMO:** By exploiting large number of antennas at the receiver (or transmitter) one can further increase the data throughput and coverage of the communication systems in a limited bandwidth. Such systems are called massive MIMO systems. Moreover, employing a large number of antennas increases the energy efficiency while simplifying the required signal processing [22].

## 2.4 Jensen's inequality

Johan Jensen proposed a very useful inequality known as Jensen's inequality in 1906. Assume  $F$  is a concave function. Let  $x_1, x_2, \dots, x_n$  be real numbers. Also, let  $a_1, a_2, \dots, a_n$  be nonnegative values so that  $\sum_{i=1}^n a_i = 1$ . We have:

$$F(a_1x_1 + \dots + a_nx_n) \geq a_1F(x_1) + \dots + a_nF(x_n). \quad (2.1)$$

---

<sup>1</sup>When different versions of the transmitted signal reach the receiver through different paths.

Also when  $F$  is a convex function, we have:

$$F(a_1x_1 + \dots + a_nx_n) \leq a_1F(x_1) + \dots + a_nF(x_n). \quad (2.2)$$

A simple proof based on induction is provided in [23] and is given below.

*Proof.* Here we only focus on the concave case. The proof for convex function is very. We use by induction.

**Basis:** Based on the definition of concave functions, for any two real valued  $x_1, x_2$  and nonnegative values  $a_1, a_2$  satisfying  $a_1 + a_2 = 1$ , we have:

$$F(a_1x_1 + a_2x_2) \geq a_1F(x_1) + a_2F(x_2). \quad (2.3)$$

**Inductive step:** Assume the statement holds for  $n$ . Then, for  $n + 1$  we have:

$$\begin{aligned} F(a_1x_1 + \dots + a_nx_n) &= F(a_1x_1 + (1 - a_1) \sum_{i=2}^{n+1} \frac{a_i}{1 - a_1} x_i) \\ &\geq a_1F(x_1) + (1 - a_1)F\left(\sum_{i=2}^{n+1} \frac{a_i}{1 - a_1} x_i\right) \end{aligned}$$

Since  $\sum_{i=2}^{n+1} \frac{a_i}{1 - a_1} = 1$  and there are  $n$  such coefficients, based on the inductive step assumption, one can extend the second term in the last equation and reach the result.  $\square$

The following example gives a better insight into Jensen's inequality.

**Example:**

Let  $F(x) = x^2$ ,  $a_1 = 0.3, a_2 = 0.5$  and  $a_3 = 0.2$ . Also assume  $x_1 = 1, x_2 = 2$

and  $x_3 = 6$ . Since  $F''(x) = 2 > 0$ ,  $F$  is a convex function. then, we have:

$$\begin{aligned} F(a_1x_1 + a_2x_2 + a_3x_3) &= F(2.5) = 6.25 \leq a_1F(x_1) + a_2F(x_2) + a_3F(x_3) \\ &= 0.3 \times 1 + 0.5 \times 4 + 0.2 \times 36 \\ &= 9.5. \end{aligned}$$

## 2.5 Arithmetic Mean-Geometric Mean Inequality

Arithmetic Mean-Geometric Mean (AM-GM) inequality is a powerful mathematical tool that is useful for solving many problems. AM-GM inequality states that for any collection of nonnegative real numbers, the geometric mean of the collection is less than or equal to their arithmetic mean. That is,

$$\frac{\sum_{i=1}^n a_i}{n} \geq \prod_{i=1}^n a_i^{\frac{1}{n}}. \quad (2.4)$$

in (2.4), the equality holds if and only if  $a_1 = a_2 = \dots = a_n$ . Next, we review a proof provided by [24].

*Proof.* According to Jensen's inequality, since the logarithmic function is concave we have:

$$\ln \sum_{i=1}^n \lambda_i a_i \geq \sum_{i=1}^n \lambda_i \ln a_i = \ln \prod_{i=1}^n a_i^{\lambda_i} \quad (2.5)$$

Using the increasing property of the logarithmic function, we get

$$\sum_{i=1}^n \lambda_i a_i \geq \prod_{i=1}^n a_i^{\lambda_i}. \quad (2.6)$$

Setting  $\lambda_i = \frac{1}{n}$  completes the proof. □

Note that the presented proof proves a more general form of AM-GM inequality ( $\sum_{i=1}^n \lambda_i a_i \geq \prod_{i=1}^n a_i^{\lambda_i}$ ) that is called weighted AM-GM inequality. The

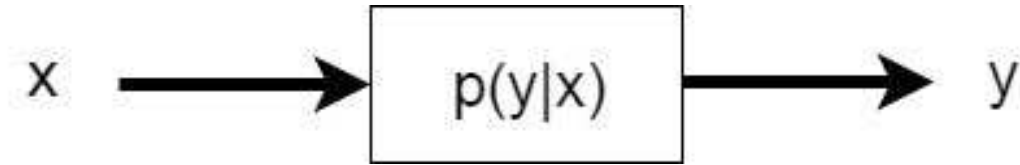


Figure 2.11: Discrete channel.

following example better illustrates AM-GM inequality.

**Example:**

Assume  $a_1 = 2, a_2 = 7, a_3 = 5$  and  $a_4 = 12$ . The arithmetic mean of this set is 6.5 and the geometric mean is 5.38. As can be seen, AM-GM inequality holds.

## 2.6 Discrete memoryless channel, Capacity and Rate

In this Section, we discuss some basic concepts which are necessary for our later discussions in the next chapter. We first start by formal definition of discrete channel. It should be note that the most of the materials in this section derived from [25].

**Definition 1.** Consider a single-input single-output system with input random variable  $X$  and output random variable  $Y$ . If  $X$  take values in a discrete subset  $\Omega$ , and  $Y$  take values in another discrete set  $\Upsilon$  such that

$$\Pr\{X = x, Y = y\} = \Pr\{X = x\}p(y|x), \quad \forall (x, y) \in \Omega \times \Upsilon \quad (2.7)$$

where  $p(y|x)$  is the transition matrix from  $\Omega$  to  $\Upsilon$ , the channel  $p(y|x)$  is called a discrete channel.

The name discrete channel comes from the fact that the input and output symbols are chosen from discrete subsets. The following definition formally defines a discrete memoryless channel [25].

**Definition 2.** Assuming instantaneous transmission, let  $X_i$  and  $Y_i$  denote the transmitted and corresponding received symbol at time  $i$ . Moreover,  $T_{i-}$  denotes all the transmitted random variable before time  $i$ . Then, the following equality holds for a discrete memoryless channel

$$\Pr\{X_i = x, Y_i = y, T_i = t\} = \Pr\{X = x, T_i = t\}p(y|x), \quad (2.8)$$

for all  $(x, y, t) \in \Omega \times \Upsilon \times \Theta$ .

That is, given the input of the channel in time  $i$ , the output of the channel is independent of the transmitted symbols before time  $i$ . This, illustrates the memoryless property of the channel.

To measure how much knowing one variable ( $X$ ) decreases uncertainty about the other variable ( $Y$ ), mutual information denoted as  $I(X; Y)$  was introduced. In other words,  $I(X; Y)$  gives the mutual information between two variables  $X$  and  $Y$  and is defined as

$$I(X; Y) = \sum_{y \in Y} \sum_{x \in X} p(x, y) \log \left( \frac{p(x, y)}{p(x)p(y)} \right). \quad (2.9)$$

For example, if  $X$  and  $Y$  are independent, then knowing one variable does not give any information about the other one, and hence the mutual information is equal to zero as  $p(x, y) = p(x)p(y)$ . In the following, the capacity of a discrete memoryless channel is given [25].

**Definition 3.** For a discrete memoryless channel with transmission matrix  $p(y|x)$ , the capacity is defined as

$$C = \sup_{p_X(x)} I(X; Y). \quad (2.10)$$

Channel capacity is measured as bits/channel-use. It can be shown that  $C$  is the maximum rate at which the information can be communicated with

small error probability [25]. The following Theorem states the channel coding theorem which defines the achievable rate for a discrete memoryless channel [25].

**Theorem 1.** *In a discrete memoryless channel, a rate  $R$  is called achievable if and only if  $R$  is equal or less than the channel capacity, i.e.  $R \leq C$ .*

Channel coding theorem states that the reliable communication is possible at any rate equal or less than the channel capacity. Next Theorem gives the capacity of a band-limited white Gaussian channel which is useful for our later discussions in Chapter 3. The proof is skipped since it is beyond the scope of this thesis.

**Theorem 2.** *The capacity of a band-limited white Gaussian channel with bandwidth  $B$  can be expressed as*

$$C = B \log_2 \left( 1 + \frac{S}{N} \right) \quad (2.11)$$

where  $\frac{S}{N}$  shows the signal-to-noise ratio (SNR),  $S$  denotes the signal power and  $N$  is the noise power.

# Chapter 3

## A General Solution For a Class of WSR and CR Maximization

### 3.1 Problem Definition

Consider  $N \geq 1$  communication links. For example  $N$  users trying to communicate with a base station or an ad-hoc network with  $N$  users. The specific communication setup of these  $N$  links is not our concern at this point. Let us denote the SNR of  $i$ -th communication link at the destination by  $\gamma_i$ . Assuming additive white Gaussian noise (AWGN), the weighted sum-rate optimization problem is defined as

$$\begin{cases} \max & \sum_{i=1}^N a_i \log_2(1 + \gamma_i) \\ \text{s.t.} & \bar{\gamma} \in \Theta, \end{cases} \quad (3.1)$$

Where  $\bar{\gamma} = (\gamma_1, \gamma_2, \dots, \gamma_n) \in \mathbb{R}^{+n}$  is the vector of communication links SNRs and  $\Theta$  is the feasible region of achievable SNRs.  $a_i$  is the weight assigned to the rate of the  $i$ -th communication link in the weighted sum rate.

The weighted sum-rate optimization problem can be further simplified as

$$\begin{cases} \max & \prod_{i=1}^N (1 + \gamma_i)^{a_i} \\ \text{s.t.} & \bar{\gamma} \in \Theta. \end{cases} \quad (3.2)$$

The weights in WSR maximization can be representative of different QoSs for different links (users).

Similarly, common-rate optimization problem in this general setup, can be expressed as

$$\begin{cases} \max & \min_i \log_2(1 + \gamma_i) \\ \text{s.t.} & \bar{\gamma} \in \Theta. \end{cases} \quad (3.3)$$

that can be simplified to

$$\begin{cases} \max & \min_i(\gamma_i) \\ \text{s.t.} & \bar{\gamma} \in \Theta. \end{cases} \quad (3.4)$$

The goal in CR maximization is to maximize the rate of the worst link. Also, in systems when all users have to transmit with the same rate, common rate maximization is equivalent to maximizing the system rate.

## 3.2 Definitions and The Proposed Solutions

### 3.2.1 Definitions

To achieve the optimal solutions of (3.2) and (3.4), we first define some useful notations.

**Definition 4.** For a given set  $B = \{b_1, b_2, \dots, b_n\} \subset \mathbb{R}^+$  we define  $\Omega_B(K)$  as the set of all points  $\mathbf{X} = (X_1, X_2, \dots, X_n) \in \mathbb{R}^{+n}$  such that

$$\sum_{i=1}^n b_i X_i \leq K,$$

where  $K \in \mathbb{R}^+$  is the greatest value that the above linear summation of  $X_i$ 's, i.e.  $\sum_{i=1}^n b_i X_i$ , can achieve.

**Definition 5.** Let  $A = \{a_1, a_2, \dots, a_n\}$  and  $B = \{b_1, b_2, \dots, b_n\}$  be non-zero finite subsets of  $\mathbb{Z}^+$  and  $\mathbb{R}^+$ , respectively, and  $K$  be a given positive constant. We define  $\vartheta_{A,B}^K = (\vartheta_{a_1, b_1}^K, \vartheta_{a_2, b_2}^K, \dots, \vartheta_{a_n, b_n}^K) \in \mathbb{R}^n$  where

$$\vartheta_{a_i, b_i}^K = \frac{a_i K}{b_i \sum_{i=1}^n a_i}, \quad \forall i \in \{1, 2, \dots, n\}.$$

One can easily show that for any arbitrary  $A \subset \mathbb{R}^+$ ,  $\vartheta_{A,B}^K \in \Omega_B(K)$ . We are now ready to propose the solutions.

### 3.2.2 The Proposed Solutions

Here we propose the main theorems and their proofs.

**Theorem 3.** Consider  $\mathbf{X} = (X_1, X_2, \dots, X_n) \in \mathbb{R}^{+n}$ ,  $\Theta \subset \Omega_B(K)$  and  $\vartheta_{A,B}^K \in \Theta$ . Then,  $\mathbf{X} = \vartheta_{A,B}^K$  is the optimal solution of the following optimization problem

$$\begin{cases} \max & \prod_{i=1}^n X_i^{a_i} \\ \text{s.t.} & \mathbf{X} \in \Theta \end{cases} \quad (3.5)$$

*Proof.* Using Definition 4 and weighted geometric-mean arithmetic-mean inequality, we have:

$$\begin{aligned} \frac{K}{\sum_{i=1}^n a_i} &\geq \frac{\sum_{i=1}^n a_i \frac{b_i X_i}{a_i}}{a} \\ &\geq \sqrt[a]{\prod_{i=1}^n \left(\frac{b_i}{a_i}\right)^{a_i} X_i^{a_i}} \end{aligned} \quad (3.6)$$

where  $a = \sum_{i=1}^n a_i$ .

Geometric-mean achieves its upper bound (arithmetic-mean) if

$$\frac{b_i X_i}{a_i} = \frac{b_j X_j}{a_j} \quad \forall i, j \in \{1, 2, \dots, n\}$$

Since we want to maximize the geometric-mean the arithmetic mean should achieve its upper bound ( $K$ ) simultaneously. Therefore,

$$\sum_{i=1}^n b_i X_i = \sum_{i=1}^n a_i \frac{b_i X_i}{a_i} = \sum_{i=1}^n a_i t = K \Rightarrow t = \frac{K}{\sum_{i=1}^n a_i},$$

which completes the proof.  $\square$

The following Theorem proposes the optimal solution for a class of optimization problems which includes common-rate optimization problems.

**Theorem 4.** *Let  $\mathbf{X} = (X_1, X_2, \dots, X_n) \in \mathbb{R}^{+n}$ ,  $\Theta \subset \Omega_B(K)$  and  $\vartheta_{A,B}^K \in \Theta$ . Then, the optimal solution of optimization problem*

$$\begin{cases} \max & \min_i(X_i) \\ \text{s.t.} & \mathbf{X} \in \Theta \end{cases} \quad (3.7)$$

is  $\mathbf{X}^{\text{opt}} = (\frac{K}{\sum_{i=1}^n b_i}, \dots, \frac{K}{\sum_{i=1}^n b_i})$  where  $b_i$ 's defined in Definition 4 if and only if  $\mathbf{X}^{\text{opt}} \in \Theta$ .

*Proof.* Simply we have:

$$\begin{aligned} \sum_{i=1}^n b_i \min \{X_i\} &\leq \sum_{i=1}^n b_i X_i \leq K \\ \min \{X_i\} &\leq \frac{K}{\sum_{i=1}^n b_i} \end{aligned} \quad (3.8)$$

To achieve the optimal solution we let  $\min \{X_i\} = \frac{K}{\sum_{i=1}^n b_i}$ .

Now if  $\exists j \in \{1, 2, \dots, n\}$   $X_j > \frac{K}{\sum_{i=1}^n b_i}$  then

$$\begin{aligned} \sum_{i=1}^n b_i X_i &\geq \sum_{i=1, i \neq j}^n b_i \min \{X_i\} + b_j X_j \\ &> \frac{K(\sum_{i=1, i \neq j}^n b_i)}{\sum_{i=1}^n b_i} + \frac{K b_j}{\sum_{i=1}^n b_i} = K \end{aligned}$$

which is a contradiction and completes the proof.  $\square$

### 3.3 Two Mathematical Examples

In this section, we present two mathematical examples to better illustrate the proposed theorems in previous section.

**Example 1:** Consider the following optimization problem

$$\left\{ \begin{array}{l} \max \quad X_1^3 X_2^2 \\ \text{s.t.} \quad 2X_1 + X_2 \leq 14 \\ \quad \quad 1 \leq X_1 \leq 6 \\ \quad \quad 2 \leq X_2 \leq 8 \end{array} \right. \quad (3.9)$$

Here, we have  $a_1 = 3, a_2 = 2, b_1 = 2, b_2 = 1$  and  $K = 14$ . Moreover,  $\Omega_B(K) = \{(X_1, X_2) \in \mathbb{R} \mid 2X_1 + X_2 \leq 14, 1 \leq X_1 \leq 6, 2 \leq X_2 \leq 8\}$ . Thus,

$$\begin{aligned} X_1^{opt} &= \vartheta_{a_1, b_1}^K = \frac{a_1 K}{b_1(a_1 + a_2)} = 4.2 \\ X_2^{opt} &= \vartheta_{a_2, b_2}^K = \frac{a_2 K}{b_2(a_2 + a_2)} = 5.6. \end{aligned}$$

Since  $\vartheta_{A,B}^K = (4.2, 5.6) \in \Omega_B(K)$ , the obtained solution is optimal.

**Example 2:** Consider another problem as

$$\begin{cases} \max & \min_i(X_i) \\ \text{s.t.} & \mathbf{X} \in \Theta \end{cases}$$

following the same procedure as Example 1 and using Theorem 4, we have

$$\begin{aligned} X_1^{opt} &= \frac{K}{b_1 + b_2} = \frac{14}{3} \\ X_2^{opt} &= \frac{K}{b_1 + b_2} = \frac{14}{3}. \end{aligned}$$

Again since  $(X_1^{opt}, X_2^{opt}) = (4.66, 4.66) \in \Omega_B(K)$ , the obtained solution is optimal.

# Chapter 4

## Applications

In this Chapter, we propose some real-world examples of massive MIMO two-way relay networks to show the practicality of the presented Theorems in Chapter 3.

### 4.1 Two-way Relay Network with Single-antenna Relay

#### 4.1.1 System model

We consider a two-way relay system including one single antenna relay  $R$  and two multiple antenna terminals  $T_a$  and  $T_b$  with  $N_a$  and  $N_b$  antennas, respectively, where  $N_a \gg N_b$ . This, for example, can be the case when a massive MIMO base station ( $T_a$ ) is communicating with a MIMO base station ( $T_b$ ) using a mobile user ( $R$ ) as relay. The channel coefficients  $\mathbf{h}_a$  and  $\mathbf{h}_b$  between  $T_a$  and  $T_b$ , and relay  $R$  are assumed to be reciprocal and independent. Moreover, additive white Gaussian noise (AWGN) with mean zero and variance  $\sigma^2$  are assumed for each link. let  $P_a$ ,  $P_b$  and  $P_r$  denote the transmit powers at the sources  $T_a, T_b$  and  $R$  respectively. The system model is shown in Fig. 4.1.

The bi-directional communication between the two terminals takes two time

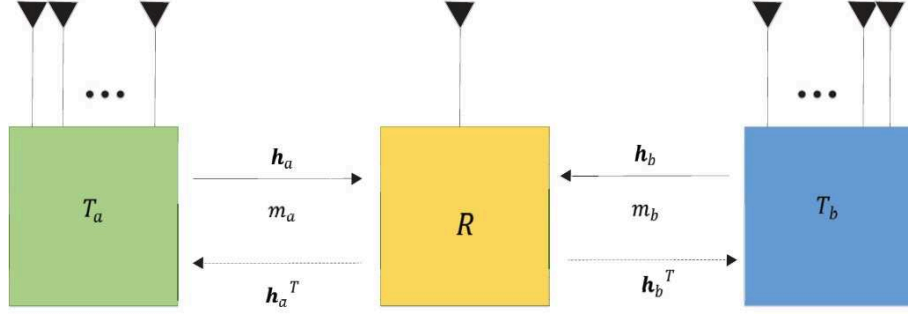


Figure 4.1: System model of a two-way relay network using multiple antennas.

slots for completion. In the first time slot, both terminals transmit to the relay. In the second time slot, the relay broadcasts the received composite signal to the two terminals. The received signal at  $R$  in the first time slot can be expressed as

$$y_r = \sqrt{P_a} \mathbf{h}_a^T \mathbf{w}_a x_a + \sqrt{P_b} \mathbf{h}_b^T \mathbf{w}_b x_b + n_r, \quad (4.1)$$

where  $x_a$  and  $x_b$  are unit energy transmit signals at the terminals and  $n_r$  is additive white gaussian noise (AWGN). With maximum ratio transmission (MRT) beamforming (see [26]), the transmit weight vectors are  $\mathbf{w}_l = (\frac{\mathbf{h}_l^\dagger}{\|\mathbf{h}_l\|})^T$ ,  $\forall l \in \{a, b\}$ . The transmit signal of the relay may be written as  $\hat{y}_r = G y_r$  where  $G = \sqrt{\frac{P_r}{P_a \|\mathbf{h}_a\|^2 + P_b \|\mathbf{h}_b\|^2 + \sigma^2}}$ , where the gain  $G$  is selected to satisfy the relay power constraint. Finally, the received signals at terminals  $T_a$  and  $T_b$ , are given by

$$y_l = \mathbf{h}_l G (\sqrt{P_l} \|\mathbf{h}_l\| x_l + \sqrt{P_c} \|\mathbf{h}_c\| x_c + n_r) + \mathbf{n}_l, \quad \forall l \in \{a, b\} \quad (4.2)$$

where  $c = \{a, b\} \setminus \{l\}$  and  $\mathbf{n}_l$  denotes the AWGN vector at terminal  $l$ . After self-interference cancellation and maximum ratio combining (MRC) (see [26]) reception with weights  $\mathbf{w}_l^T = (\frac{\mathbf{h}_l^\dagger}{\|\mathbf{h}_l\|})$ ,  $\forall l \in \{a, b\}$ , the received signals at both

terminals can be expressed as

$$\hat{y}_l = G\sqrt{P_c}\|\mathbf{h}_l\|\|\mathbf{h}_c\|x_c + G\|\mathbf{h}_l\|n_r + \hat{n}_l, \forall l \in \{a, b\} \quad (4.3)$$

where  $\hat{n}_l = \frac{\mathbf{h}_l^\dagger \mathbf{n}_l}{\|\mathbf{h}_l\|}$ ,  $\forall l \in \{a, b\}$ . Using (4.3), the SNRs at the two terminals can be obtained as

$$\gamma_l = \frac{P_c P_r}{\sigma^2} \left[ \frac{\|\mathbf{h}_c\|^2 \|\mathbf{h}_l\|^2}{(P_l + P_r)\|\mathbf{h}_l\|^2 + P_c\|\mathbf{h}_c\|^2 + \sigma^2} \right], \forall l \in \{a, b\} \quad (4.4)$$

### 4.1.2 Problem Formulation

Restricting the total power consumed below a threshold is one way to control the total interference of this network on neighbouring networks. The total power constraint has also been considered in [18, 27–29]. Therefore, we maximize the achievable sum rate of the system subject to a total power constraint, which can be formulated as

$$\begin{aligned} & \max_{P_a, P_b, P_r} \mathbf{R} \\ \text{s.t.} \quad & P_a + P_b + P_r = P_t, \end{aligned} \quad (\text{P1})$$

where  $\mathbf{R} = \frac{1}{2} \log_2(1 + \gamma_a) + \frac{1}{2} \log_2(1 + \gamma_b)$ . Since  $\log(x)$  is an increasing function, by combining the two log terms, we can reformulate (P1) as

$$\begin{aligned} & \max_{P_a, P_b, P_r} (1 + \gamma_a)(1 + \gamma_b) \\ \text{s.t.} \quad & P_a + P_b + P_r = P_t, \end{aligned} \quad (\text{P2})$$

### 4.1.3 Optimal Power Allocation

In the following, we give the exact solution:

**Theorem 1.** For massive antenna users, the optimal power allocation of (P2)

is

$$P_a = \frac{P_t}{2(\sqrt{\nu} + 1)} \quad , \quad P_b = \frac{P_t\sqrt{\nu}}{2(\sqrt{\nu} + 1)} \quad , \quad P_r = \frac{P_t}{2} \quad (4.5)$$

where  $\nu = \frac{\gamma_{ar}}{\gamma_{br}}$ ,  $\gamma_{ar} = \frac{P_t}{\sigma^2} \|\mathbf{h}_a\|^2$  and  $\gamma_{br} = \frac{P_t}{\sigma^2} \|\mathbf{h}_b\|^2$ .

*Proof.* We rewrite the total power constraint  $P_a + P_b + P_r = P_t$  with two auxiliary variables  $\alpha$  and  $\beta$  such  $P_a = \alpha\beta P_t$ ,  $P_b = (1-\alpha)\beta P_t$  and  $P_r = (1-\beta)P_t$  ( $0 \leq \alpha, \beta \leq 1$ ). We need to find the optimal value of  $\alpha$  and  $\beta$ . Now, (P2) is a special case of problem (3.5) with  $n = 2$ ,  $X_1 = 1 + \gamma_a$ ,  $X_2 = 1 + \gamma_b$  and  $a_1 = a_2 = 1$ . Using Theorem 3, one can easily show that for  $\nu \gg 1$ , if  $\gamma_a^{opt} = \gamma_b^{opt} = \frac{\gamma_{br}}{2 + 4\sqrt{\frac{1}{\nu}}}$  is in the feasibility region then the corresponding power allocation is optimal. Hence, we only need to show that

$$\gamma_a^{opt} = \gamma_b^{opt} = \frac{\gamma_{br}}{2 + 4\sqrt{\frac{1}{\nu}}} \quad (4.6)$$

is feasible. This is equivalent to showing that  $0 \leq \alpha^{opt}, \beta^{opt} \leq 1$ . The corresponding  $\alpha, \beta$  can be obtained as:

$$\alpha^{opt} = \frac{1}{\sqrt{\nu} + 1} \quad , \quad \beta^{opt} = \frac{1}{2} \quad (4.7)$$

which both satisfy  $0 \leq \alpha^{opt}, \beta^{opt} \leq 1$ . □

It is interesting to see that the optimal allocation requires that half of the total power be allocated to the relay and the remaining half is divided according to the ratio  $1 : \sqrt{\nu}$ . Since  $\nu$  is large, more power is thus allocated to  $T_b$ . Note that  $\nu$  (4.5) is a random variable. However, since one of the terminals is massive MIMO, by using the weak-law of large numbers, we approximate it as  $\nu \simeq \frac{N_a\sigma_a^2}{N_b\sigma_b^2}$ . The details of the approximation are detailed in (4.9), and numerical evidence for its accuracy is given in Section 4.1.6. This constant

value is used for the ergodic sum rate analysis next.

#### 4.1.4 Ergodic sum rate

While the optimal solution derived in (4.5) yields the instantaneous total sum rate as a function of instantaneous channel gains, the ergodic sum rate, a far more important performance measure, is derived by averaging over all channel statistics. For this purpose, all the entries in the channel vectors  $\mathbf{h}_a$  and  $\mathbf{h}_b$  between  $T_a$  and  $T_b$ , and relay  $R$  are assumed to be independent and Nakagami- $m$  distributed with parameters  $m_a, m_b \in \mathbb{N}$  and average fading powers  $\sigma_a$  and  $\sigma_b$ , respectively. Therefore, our results also include Rayleigh fading channels as a special case when  $m_a = m_b = 1$ .

**Theorem 2.** The ergodic sum rate for the optimal PA obtained in Theorem 1 can be expressed as

$$\bar{\mathbf{R}} = s(2 + 4\sqrt{\frac{1}{\nu}})^{m_b N_b} \exp\left(\frac{m_b(2 + 4\sqrt{\frac{1}{\nu}})}{\bar{\gamma}_{br}}\right) \sum_{k=1}^{m_b N_b} \frac{\Gamma\left(k - m_b N_b, \frac{m_b(2 + 4\sqrt{\frac{1}{\nu}})}{\bar{\gamma}_{br}}\right)}{\left(\frac{m_b(2 + 4\sqrt{\frac{1}{\nu}})}{\bar{\gamma}_{br}}\right)^k} \quad (4.8)$$

where  $s = \frac{(m_b N_b - 1)!}{\ln 2 \Gamma(m_b N_b)} \left(\frac{m_b}{\bar{\gamma}_{br}}\right)^{m_b N_b}$ .

*Proof.* Using the weak-law of large numbers,  $\frac{\sum_{i=1}^{N_l} |h_{li}|^2}{N_l} \xrightarrow{p} \mathbf{E}(|h_l|^2) = \sigma_l^2$  as  $N_l \rightarrow \infty$ ,  $\forall l \in \{a, b\}$  where  $\xrightarrow{p}$  denotes the convergence in probability. Hence:

$$\nu = \frac{N_a \frac{\sum_{i=1}^{N_a} |h_{ai}|^2}{N_a}}{N_b \frac{\sum_{k=1}^{N_b} |h_{bk}|^2}{N_b}} = \frac{N_a \sigma_a^2}{N_b \sigma_b^2} \quad (4.9)$$

However, even for small number of antennas, this approximation is good (see

Section 4.1.6). To evaluate the ergodic sum rate,  $\bar{\mathbf{R}} = \frac{1}{2}E[\log_2(1 + \gamma_a) + \log_2(1 + \gamma_b)] = E[\log_2(1 + \gamma_a)]$ , we have:

$$\begin{aligned}
\bar{\mathbf{R}} &= E[\log_2(1 + \gamma_a)] \\
&= \int_0^\infty \int_0^\infty \log_2(1 + \gamma_a) f(\gamma_{ar}, \gamma_{br}) d\gamma_{ar} d\gamma_{br} \\
&\stackrel{(a)}{=} \int_0^\infty \int_0^\infty \log_2(1 + \gamma_a) f_{\gamma_{ar}}(\gamma_{ar}) f_{\gamma_{br}}(\gamma_{br}) d\gamma_{ar} d\gamma_{br} \\
&\stackrel{(b)}{\simeq} \int_0^\infty \log_2(1 + \gamma_a) f_{\gamma_{br}}(\gamma_{br}) d\gamma_{br} \\
&\stackrel{(c)}{=} \frac{1}{\ln 2 \Gamma(m_b N_b)} \left(\frac{m_b}{\bar{\gamma}_{br}}\right)^{m_b N_b} \int_0^\infty \ln\left(1 + \frac{\gamma_{br}}{2 + 4\sqrt{\frac{1}{\nu}}}\right) \gamma_{br}^{m_b N_b - 1} \exp\left(-\frac{m_b \gamma_{br}}{\bar{\gamma}_{br}}\right) d\gamma_{br} \\
&\stackrel{(d)}{=} \frac{(2 + 4\sqrt{\frac{1}{\nu}})^{m_b N_b} (m_b N_b - 1)!}{\ln 2 \Gamma(m_b N_b)} \left(\frac{m_b}{\bar{\gamma}_{br}}\right)^{m_b N_b} \times \\
&\quad \exp\left(-\frac{m_b(2 + 4\sqrt{\frac{1}{\nu}})}{\bar{\gamma}_{br}}\right) \sum_{k=1}^{m_b N_b} \frac{\Gamma\left(k - m_b N_b, \frac{m_b(2 + 4\sqrt{\frac{1}{\nu}})}{\bar{\gamma}_{br}}\right)}{\left(\frac{m_b(2 + 4\sqrt{\frac{1}{\nu}})}{\bar{\gamma}_{br}}\right)^k}
\end{aligned} \tag{4.10}$$

where:

(a) follows from the fact that two channel hops are independent.

(b) follows from the fact that  $\gamma_a$  is independent from  $\gamma_{ar}$ .

(c) the reason is that channel coefficients follow Nakagami-m distribution.

(d) follows from the fact that  $\int_0^\infty \ln(1+x)x^{n-1} \exp(-tx)dx = (n-1)!e^t \sum_{k=1}^n \frac{\Gamma(-n+k,t)}{t^k}$  for  $t > 0$ ,  $n = 1, 2, \dots$  [30, Appendix B].  $\square$

## 4.1.5 Additional QoS constraints

In this part, we add more realistic QoS constraints to the previous problem and try to solve it. We propose a sub-optimal solution for the new problem, and we show that the proposed solution outperforms the conventional power allocation solutions.

## Problem Formulation

Suppose, in comparison to the SNRs they have achieved in (4.6), one of the terminals needs a higher SNR (e.g., for better quality of service) while the other one does not. This scenario is of interest in wireless cellular networks where some mobile users may require higher SNRs due to limitations such as hardware requirements. In below, we treat the case where it is Terminal  $T_b$  that needs higher SNR out of the two terminals.

In this scenario, we maximize the sum rate subject to the constraints that the total power of the network is  $P_t$  and the SNRs at both terminals must exceed target threshold values. Therefore, the optimization problem (P2) can be reformulated as

$$\begin{aligned}
 & \max_{P_a, P_b, P_r} \mathbf{R} \\
 \text{s.t. } & P_a + P_b + P_r = P_t \\
 & \gamma_a \geq \hat{\gamma}_a \\
 & \gamma_b \geq \hat{\gamma}_b
 \end{aligned} \tag{P3}$$

where  $\hat{\gamma}_b > \gamma_b^{opt}$ .

## Sub-Optimal Solution

In order to solve (P3), we first note that with the optimal power allocation (4.5), both terminals reach SNRs approximately  $\frac{\gamma_{br}}{2}$  as  $\nu \rightarrow \infty$ . From a practical point of view, since  $T_a$  and  $T_b$  can be considered as base station and mobile user, respectively, it makes sense to increase the SNR of the mobile terminal ( $T_b$ ), who has the fewer number of antennas. To quantify the SNR improvement, we define an improvement coefficient  $\hat{\gamma}_b = \zeta \frac{\gamma_{br}}{2}$  where  $1 \leq \zeta \leq 2$ .

To achieve a sub-optimal solution for this case, we set the SNR of  $T_b$ , which requires higher SNR, to the target value and maximize the SNR of  $T_a$ . So, let

$\gamma_b = \frac{\alpha\beta(1-\beta)\gamma_{ar}}{\alpha\beta\nu+1} = \hat{\gamma}_b$  then we have

$$\alpha = \frac{\hat{\gamma}_b}{\beta(1-\beta)\gamma_{ar} - \beta\nu\hat{\gamma}_b}. \quad (4.11)$$

To simplify the analysis, let  $\nu \gg 1$  which is equivalent to exploiting large scale antenna arrays at terminal  $T_a$ . Therefore, we have

$$\gamma_a(\beta) \simeq \beta\gamma_{br} - \frac{\hat{\gamma}_b\gamma_{br}}{\gamma_{ar}(1-\beta-\frac{\hat{\gamma}_b}{\gamma_{br}})}, \quad (4.12)$$

By taking derivative of  $\gamma_a(\beta)$  with respect to  $\beta$ , we obtain

$$\beta^{s-opt} = 1 - \sqrt{\frac{\hat{\gamma}_b}{\gamma_{ar}} - \frac{\hat{\gamma}_b}{\gamma_{br}}}, \quad (4.13)$$

Because  $0 < \beta^{s-opt} < 1$ , we have  $0 < \sqrt{\frac{\hat{\gamma}_b}{\gamma_{ar}} + \frac{\hat{\gamma}_b}{\gamma_{br}}} < 1$ . The second inequality should be considered as the feasibility condition. By substituting  $\beta^{s-opt}$  in (4.11), one can easily show that  $0 < \alpha < 1$ . Using  $\beta^{s-opt}$ , we obtain

$$\gamma_a^{s-opt} = \gamma_{br} - \hat{\gamma}_b - 2\gamma_{br}\sqrt{\frac{\hat{\gamma}_b}{\gamma_{ar}}}. \quad (4.14)$$

### Ergodic Sum Rate

We next provide the closed-form ergodic sum rate over Nakagami-m fading channels for the solutions given in (4.11) and (4.13).

**Theorem 3.** The ergodic sum rate for the sub-optimal solutions given in (4.11) and (4.13), can be expressed as

$$\bar{\mathbf{R}} = \sum_{i \in \mathcal{C}} s_i^{m_b N_b} \exp\left(\frac{m_b i}{\bar{\gamma}_{br}}\right) \sum_{k=1}^{m_b N_b} \frac{\Gamma\left(k - m_b N_b, \frac{m_b i}{\bar{\gamma}_{br}}\right)}{\left(\frac{m_b i}{\bar{\gamma}_{br}}\right)^k}, \quad (4.15)$$

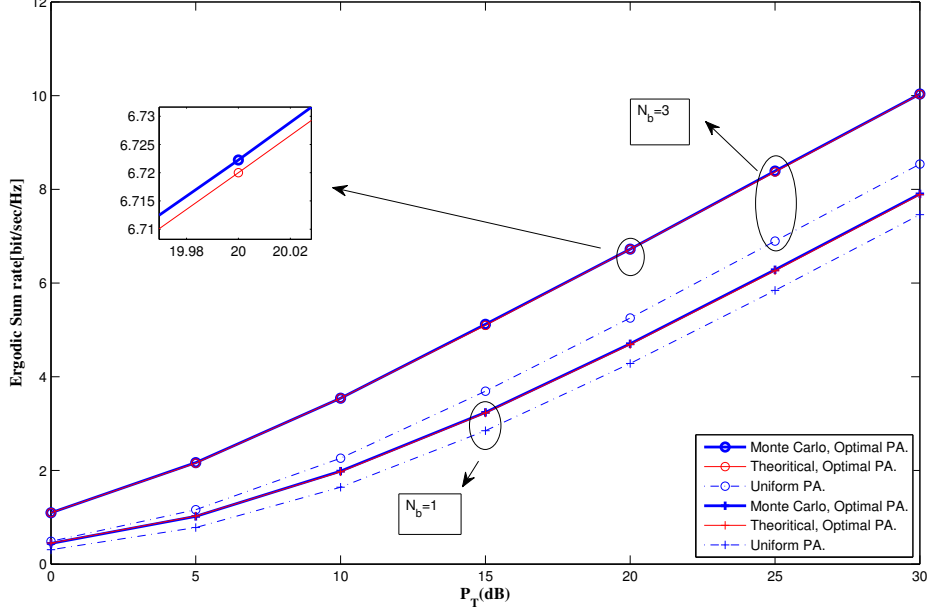


Figure 4.2: Achievable sum rate performance using PPA and UPA with  $\nu = 100$ ,  $\sigma_a^2 = \sigma_b^2 = 1$ ,  $m_b = 1$  and  $N_0 = 1$ .

where  $C = \left\{ \frac{1}{1 - \frac{\zeta}{2} - 2\sqrt{\frac{\zeta}{2\nu}}}, \frac{2}{\zeta} \right\}$  and  $s$  is given in (4.8).

*Proof.* First, one should notice that  $1 \leq \zeta < 2$  where the upper bound comes from the domain of logarithm function. Using this fact and equations (4.11) and (4.13), the ergodic sum rate expression for the presented sub-optimal power allocation can be proven similar to proof of Theorem 2.  $\square$

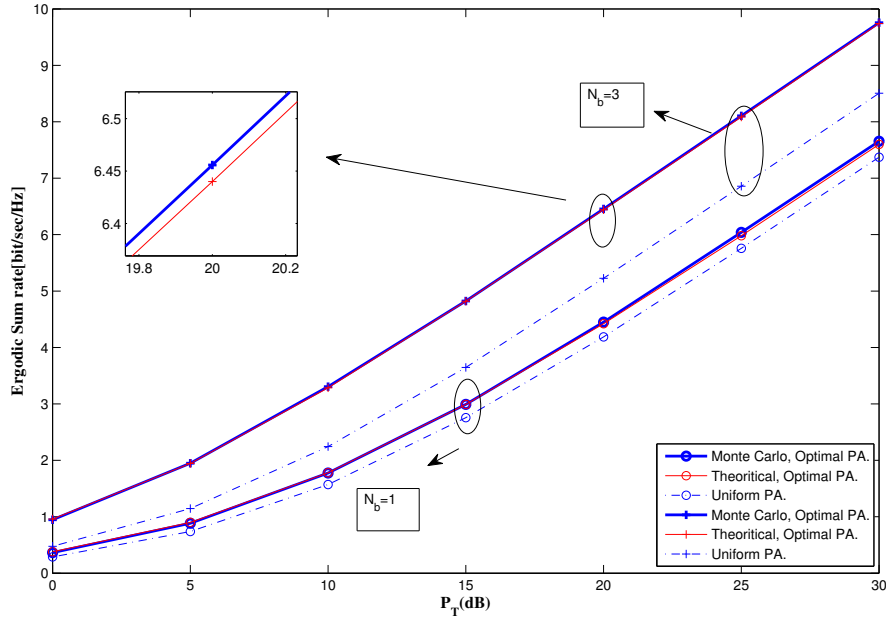


Figure 4.3: Achievable sum rate performance using PPA and UPA with  $\nu = 20$ ,  $\sigma_a^2 = \sigma_b^2 = 1$  and  $m_b = 1$ .

#### 4.1.6 Numerical And Simulation Results

In this section, Monte Carlo simulation results and theoretical analyses given in (4.5) and (4.15) are compared for verification.

Figs. 4.2 and 4.3 show the ergodic sum rate of both optimal PA and uniform power allocation (UPA) ( $P_a = P_b = P_r = P_t/3$ ) for different values  $\nu = 100, 20$  and  $N_b = 1, 3$ . These figures show the following:

- 1) The analytical result (4.8) agrees well with the Monte Carlo simulations, even for lower values of  $\nu = 20$ .
- 2) The optimal PA offers better ergodic sum rates over the UPA. For example, for  $\nu = 100$ ,  $N_b = 1$  and  $\bar{\mathbf{R}} = 4$  bit/s/Hz, a 1 dB gap exists between (4.8) and UPA. Moreover, as the antennas of  $T_b$  increases to 3, this gap increases to about 5 dB.

Fig. 4.4, illustrates the impact of  $\nu$  on the system ergodic sum rate for both (4.8) and UPA. As can be seen, optimal PA outperforms UPA for different values of  $\nu$ .

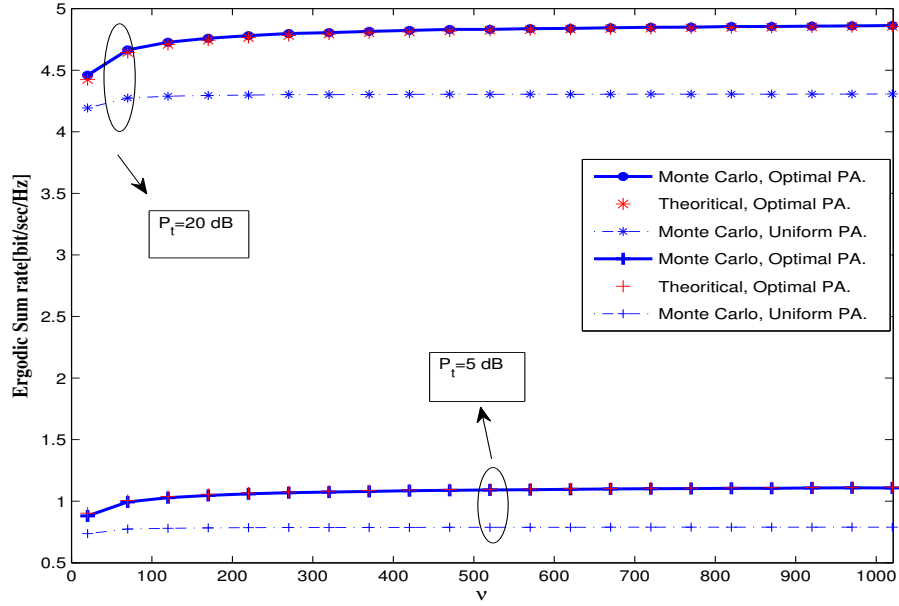


Figure 4.4: Impact of  $\nu$  on the achievable sum rate with  $\sigma_a^2 = \sigma_b^2 = 1$ ,  $m_b = 1$ ,  $N_0 = 1$  and  $N_b = 1$ .

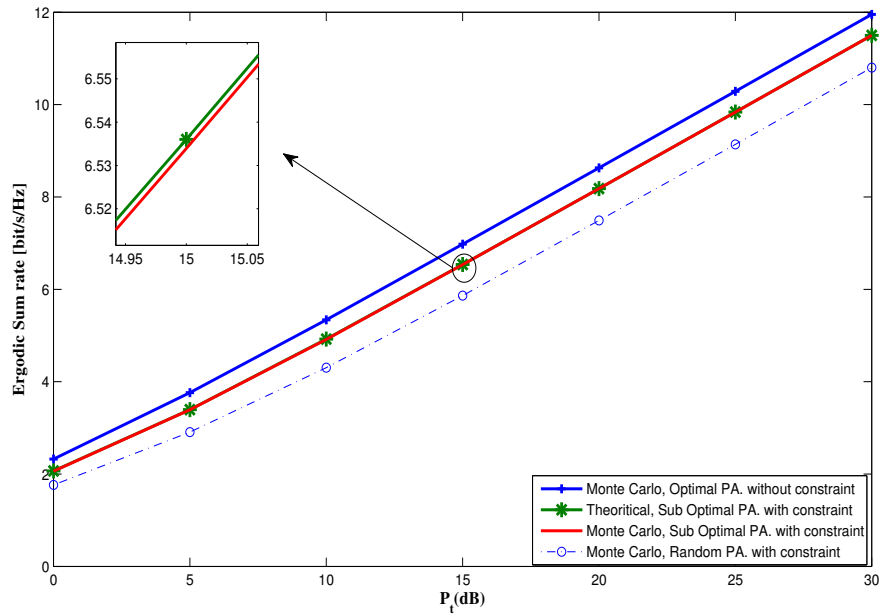


Figure 4.5: The achievable sum rate of Sub-Optimal PA for a feasible system with  $\sigma_a^2 = \sigma_b^2 = 1$ ,  $m_b = 1$ ,  $N_0 = 1$ ,  $N_b = 10$ ,  $\zeta = 1.4$  and  $\nu = 100$ .

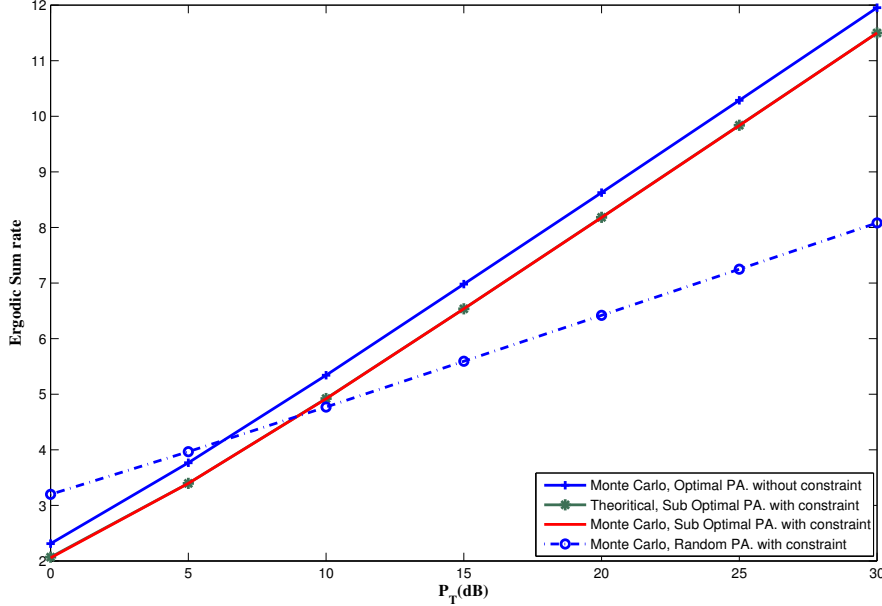


Figure 4.6: The achievable sum rate of Sub-Optimal PA for an infeasible system with  $\sigma_a^2 = \sigma_b^2 = 1$ ,  $m_b = 1$ ,  $N_0 = 1$ ,  $N_b = 10$ ,  $\zeta = 1.4$  and  $\nu = 100$ .

Fig. 4.5 shows that the simulation results match well with theoretical expression (4.15). Furthermore, the proposed sub-optimal power allocation outperforms random PA which satisfies considered QoS constraints. For example, for  $\nu = 100$ ,  $N_b = 10$  and  $\bar{\mathbf{R}} = 4$  bit/s/Hz, the sub-optimal power allocation strategy saves the total power about 2 dB in comparison with random PA.

In Fig. 4.6,  $\hat{\gamma}_a$  is set so that the system becomes infeasible. It is clear that the sum rate for random PA is even greater than the PPA in low powers. In this case, the system cannot provide the target SNR due to total power constraint. However, when the systems becomes feasible, the presented sub-optimal power allocation strategy outperforms the random PA.

As shown in Fig. 4.5 and Fig. 4.6, the derived sub-optimal solution is close to the optimal solution of the first scenario which is a relaxed version of the second scenario. Hence, the proposed sub-optimal solution is even closer to the optimal solution of its own setup.

Finally, all the figures verify that the approximation  $\nu \simeq \frac{N_a \sigma_a^2}{N_b \sigma_b^2}$  results in

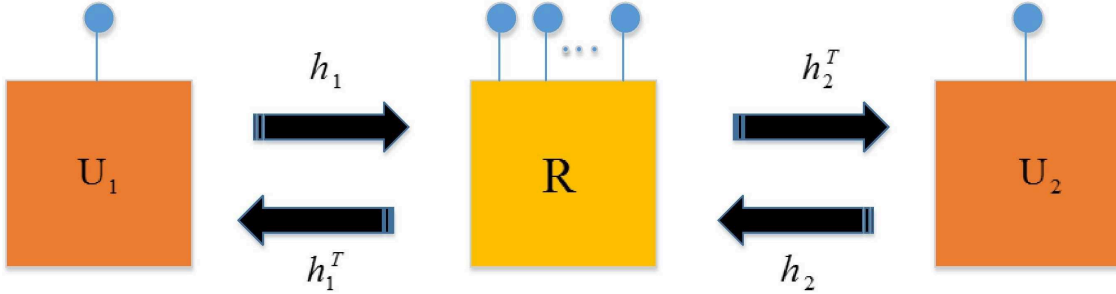


Figure 4.7: The system model of a two-way relay network using multiple-antenna relay.

the ergodic sum rate expressions that match well with the simulation results.

## 4.2 Two-way Relay Network with Multiple-antenna Relay

In this section, to show the usefulness of the developed framework, we propose another bidirectional (two-way) relay example. To the best of our knowledge, the optimization results that we present are novel and have not appeared in the literature.

### 4.2.1 System model

We consider a network (Fig. 4.7) consisting of one two-way relay which is equipped with  $N_r \geq 1$  antennas and two single-antenna users  $U_1$  and  $U_2$ . The channel coefficients for the two links  $U_1 \leftrightarrow R$  and  $U_2 \leftrightarrow R$  are  $\mathbf{h}_1$  and  $\mathbf{h}_2$ , respectively. These channels are assumed to be reciprocal and the coefficients are independent. The transmit powers for users  $U_1$ ,  $U_2$  and relay  $R$  are denoted by  $P_1$ ,  $P_2$  and  $P_r$ , respectively. Moreover, we assume AWGN with mean zero and variance  $\sigma^2$  for each hop. The communication protocol involves three time slots and is as follows.

In the first time slot, both users transmit their signals to the relay. In the

second time slot, the relay amplifies (with gain  $G$ ) and employs maximal ratio transmission beamforming with weight  $\mathbf{w}_1 = \frac{\mathbf{h}_1^* \mathbf{h}_2^\dagger}{\|\mathbf{h}_1\| \|\mathbf{h}_2\|}$  to forward the combined signals to  $U_1$ . In the third time slot, relay follows the same procedure as the second time slot, with weight  $\mathbf{w}_2 = \frac{\mathbf{h}_2^* \mathbf{h}_1^\dagger}{\|\mathbf{h}_1\| \|\mathbf{h}_2\|}$ , to forward the received signal to  $U_2$ . Therefore, the received signal at  $R$  is given by:

$$y_r = \sqrt{P_1} \mathbf{h}_1 x_1 + \sqrt{P_2} \mathbf{h}_2 x_2 + \mathbf{n}_r, \quad (4.16)$$

where  $x_1$  and  $x_2$  are unit energy transmit signals and  $\mathbf{n}_r$  is the relay AWGN term. The relay gain is

$$G = \sqrt{\frac{P_r}{P_1 \|\mathbf{h}_1\|^2 + P_2 \|\mathbf{h}_2\|^2 + \sigma^2}}$$

Using the transmission weight vectors and after self-interference cancellation by each user, the received signal at  $U_1$  and  $U_2$  can be expressed as:

$$\begin{aligned} \hat{y}_1 &= G \sqrt{P_2} \|\mathbf{h}_1\| \|\mathbf{h}_2\| x_2 + n_1 + \hat{n}_1 \\ \hat{y}_2 &= G \sqrt{P_1} \|\mathbf{h}_2\| \|\mathbf{h}_1\| x_1 + n_2 + \hat{n}_2, \end{aligned} \quad (4.17)$$

where  $\hat{n}_1 = k \mathbf{w}_1 \mathbf{h}_1^T \mathbf{n}_r$ ,  $\hat{n}_2 = k \mathbf{w}_2 \mathbf{h}_2^T \mathbf{n}_r$  and  $n_1, n_2$  are the AWGN noises at users  $U_1$  and  $U_2$ , respectively. Using (4.17), one can easily show that the SNRs at the receiver of each user are given by:

$$\begin{aligned} \gamma_2 &= \frac{P_1 P_r}{\sigma^2} \left[ \frac{\|\mathbf{h}_1\|^2 \|\mathbf{h}_2\|^2}{(P_2 + P_r) \|\mathbf{h}_2\|^2 + P_1 \|\mathbf{h}_1\|^2 + \sigma^2} \right] \\ \gamma_1 &= \frac{P_2 P_r}{\sigma^2} \left[ \frac{\|\mathbf{h}_1\|^2 \|\mathbf{h}_2\|^2}{(P_1 + P_r) \|\mathbf{h}_1\|^2 + P_2 \|\mathbf{h}_2\|^2 + \sigma^2} \right]. \end{aligned} \quad (4.18)$$

## 4.2.2 Common-rate

We need to maximize the common-rate subject to the total power constraint.

This problem can be formulated as

$$\begin{cases} \max_{P_1, P_2, P_r} & \min(\gamma_1, \gamma_2) \\ \text{s.t.} & P_1 + P_2 + P_r \leq P_t. \end{cases} \quad (4.19)$$

We next provide a proposition in order to reformulate optimization problem (4.19).

**Proposition 1.** The constraint  $P_1 + P_2 + P_r \leq P_t$  is equivalent to

$$\gamma_1 + \gamma_2 \leq \frac{\gamma_{1r}\gamma_{2r}}{(\sqrt{\gamma_{1r} + 1} + \sqrt{\gamma_{2r} + 1})^2},$$

where  $\gamma_{k,r} = \frac{P_t}{\sigma^2} \|\mathbf{h}_k\|^2$ ,  $k = 1, 2$ .

*Proof.* We can define  $P_1 = \alpha\beta P_t$ ,  $P_2 = (1 - \alpha)\beta P_t$  and  $P_r = (1 - \beta)P_t$  with  $(0 \leq \alpha, \beta \leq 1)$ . By substituting these definitions into the objective function  $f(\alpha, \beta) = \gamma_1 + \gamma_2$  and forming the equations  $\frac{\partial f}{\partial \beta} = 0$  and  $\frac{\partial f}{\partial \alpha} = 0$ , the global maximum of function  $f(\alpha, \beta)$  can be obtained as  $\frac{\gamma_{1r}\gamma_{2r}}{(\sqrt{\gamma_{1r} + 1} + \sqrt{\gamma_{2r} + 1})^2}$ .  $\square$

Hence, the problem (4.19) is equivalent to the following:

$$\begin{cases} \max_{(\gamma_1, \gamma_2) \in \Theta} & \min(\gamma_1, \gamma_2) \\ \text{s.t.} & \Theta \subset \Omega_B\left(\frac{\gamma_{1r}\gamma_{2r}}{(\sqrt{\gamma_{1r} + 1} + \sqrt{\gamma_{2r} + 1})^2}\right), \end{cases} \quad (4.20)$$

which is a special case of Theorem 4.

We present the optimal solution for problem (4.20) using Theorem 4 and show that the solution is in the subset  $\Theta$  and therefore, is feasible.

Using Theorem 4, one can show that the optimal solution is

$$\begin{aligned}\gamma_1 &= \frac{\gamma_{1r}\gamma_{2r}}{2(\sqrt{\gamma_{1r}+1} + \sqrt{\gamma_{2r}+1})^2} \\ \gamma_2 &= \frac{\gamma_{1r}\gamma_{2r}}{2(\sqrt{\gamma_{1r}+1} + \sqrt{\gamma_{2r}+1})^2},\end{aligned}$$

which results in

$$\begin{aligned}\beta^{opt} &= 0.5 \\ \alpha^{opt} &= \frac{-\gamma_{2r} - 1 + \sqrt{(\gamma_{2r}+1)(\gamma_{1r}+1)}}{\gamma_{1r} - \gamma_{2r}},\end{aligned}$$

where both of them satisfy  $0 \leq \alpha, \beta \leq 1$ . Substituting  $\beta^{opt}$  and  $\alpha^{opt}$  into  $P_1, P_2, P_r$ , we have:

$$\begin{aligned}P_1 &= \frac{P_t \left( -\gamma_{2r} - 1 + \sqrt{(\gamma_{2r}+1)(\gamma_{1r}+1)} \right)}{2(\gamma_{1r} - \gamma_{2r})} \\ P_2 &= \frac{P_t \left( \gamma_{1r} + 1 - \sqrt{(\gamma_{2r}+1)(\gamma_{1r}+1)} \right)}{2(\gamma_{1r} - \gamma_{2r})} \\ P_r &= \frac{P_t}{2}\end{aligned}\tag{4.21}$$

where  $\gamma_{1r} = \frac{P_t}{\sigma^2} \|\mathbf{h}_1\|^2$ ,  $\gamma_{2r} = \frac{P_t}{\sigma^2} \|\mathbf{h}_2\|^2$ .

### 4.2.3 Weighted sum-rate

Here we aim to maximize the weighted sum-rate of the system (Fig. 4.7) subject to the total power constraint. The weighted sum-rate can be expressed as

$$\begin{aligned}R &= \frac{a_1}{2} \log_2(1 + \gamma_1) + \frac{a_2}{2} \log_2(1 + \gamma_2) \\ &= \frac{1}{2} \log_2[(1 + \gamma_1)^{a_1} (1 + \gamma_2)^{a_2}]\end{aligned}\tag{4.22}$$

Hence, the maximization problem can be reformulated as

$$\begin{cases} \max_{P_1, P_2, P_r} & (1 + \gamma_1)^{a_1} (1 + \gamma_2)^{a_2} \\ \text{s.t.} & P_1 + P_2 + P_r \leq P_t, \end{cases} \quad (4.23)$$

Using Proposition 1, optimization problem (4.23) turns to

$$\begin{cases} \max_{(1+\gamma_1, 1+\gamma_2) \in \Theta} & (1 + \gamma_1)^{a_1} (1 + \gamma_2)^{a_2} \\ \text{s.t.} & \Theta \subset \Omega_B \left( 2 + \frac{\gamma_{1r} \gamma_{2r}}{(\sqrt{\gamma_{1r} + 1} + \sqrt{\gamma_{2r} + 1})^2} \right), \end{cases} \quad (4.24)$$

which is a special case of Theorem 3.

From Theorem 3, the optimal solution of (4.24) occurs when

$$\begin{aligned} \gamma_1 &= \frac{a_1 - a_2}{a_1 + a_2} + \frac{a_1}{a_1 + a_2} \left( \frac{\gamma_{1r} \gamma_{2r}}{(\sqrt{\gamma_{1r} + 1} + \sqrt{\gamma_{2r} + 1})^2} \right) \\ \gamma_2 &= \frac{a_2 - a_1}{a_1 + a_2} + \frac{a_2}{a_1 + a_2} \left( \frac{\gamma_{1r} \gamma_{2r}}{(\sqrt{\gamma_{1r} + 1} + \sqrt{\gamma_{2r} + 1})^2} \right) \end{aligned}$$

For instance, assuming  $a_1 = 2$ ,  $a_2 = 1$ ,  $P_t = 0$  dB,  $N_r = 100$ ,  $\gamma_{1r} = 24$ , and  $\gamma_{2r} = 96$ , the optimal solution will be  $\gamma_1 = 7.3$  and  $\gamma_2 = 3.15$  which translates to  $P_1 = 0.1996$ ,  $P_2 = 0.2362$  and  $P_r = 0.5642$ .

#### 4.2.4 Numerical And Simulation Results

In this section, we present simulation results to verify the optimality of the solutions given by Theorems 3 and 4.

In Figs. 4.8 and 4.9, we have plotted the achievable common-rate and weighted sum-rate of the considered system model for the presented solutions in Section 4.2. To verify the optimality of these results, we also present the solution which has been obtained through searching (with step 0.001) the feasible SNR region. This has been performed for two cases of  $N_r = 16$  and  $N_r = 100$ . Furthermore, as a benchmark, the achievable common-rate of uniform power

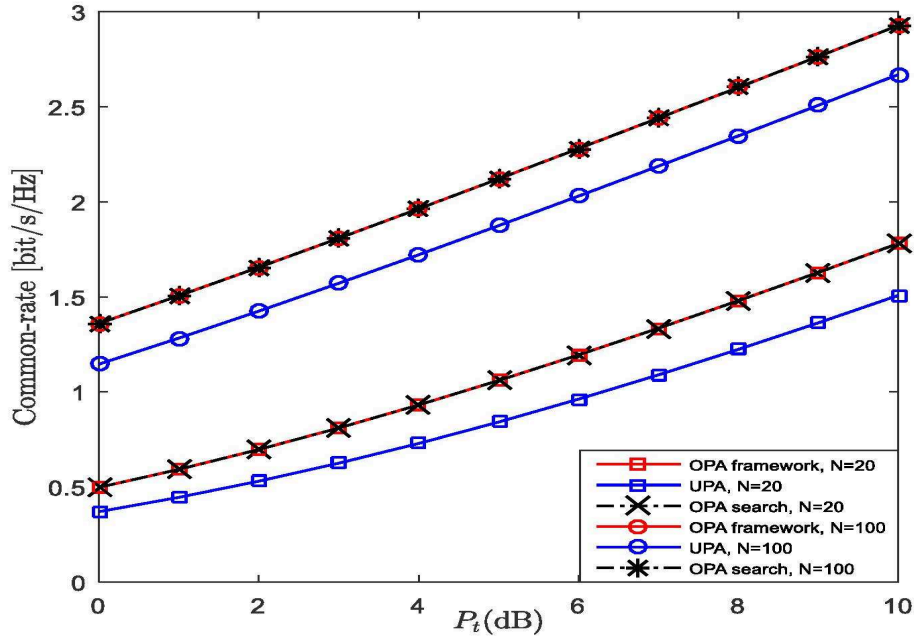


Figure 4.8: Achievable common-rate  $a_1 = 2, a_2 = 1, \sigma_1^2 = 0.25, \sigma_2^2 = 1$  and  $\sigma^2 = 1$ .

allocation (UPA) has also been plotted. As can be seen, the theoretical results match well with the search method solutions in both cases. Moreover, as expected, the optimal power allocations outperform the UPA.

### 4.3 Case Study: [ShahbazPanahi et al., 2012]

Here, the problem considered in [18] is briefly discussed to further demonstrate the applicability of the proposed Theorems in Chapter 3.

A similar problem to (P2) has been considered in [18]. The only difference is the transceivers and relay are all equipped with single antenna, . The authors in [18] have shown the rate region achieved by the two transceivers is triangular. The following remarks re-obtain the results achieved in [18] using the presented Theorems in Chapter 3.

**Remark 1.** For the rate region  $\Theta$  obtained in [18],  $K = 2 + 2\gamma_{max}$ ,  $b_i = 1 \forall i \in \{1, 2\}$ , using Theorem 3, the optimal solution for maximizing the sum-

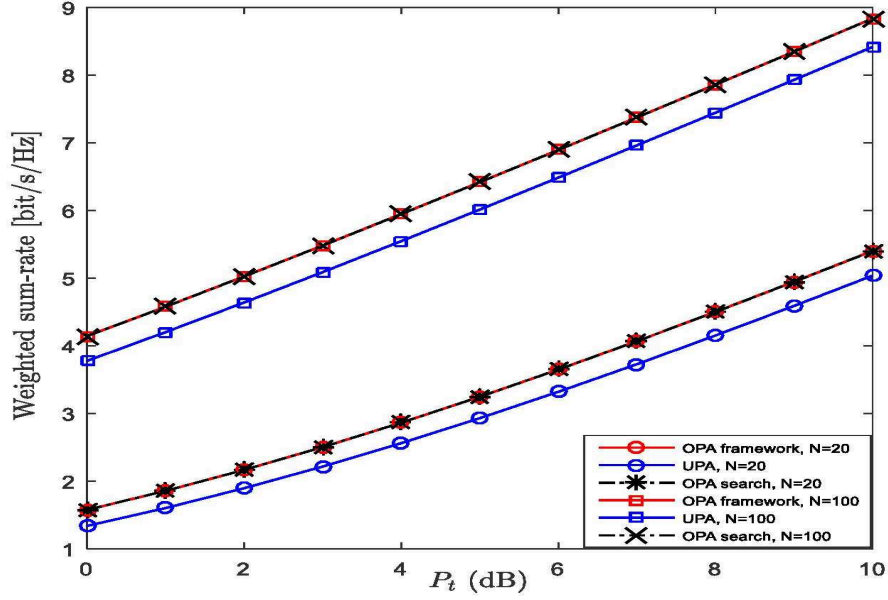


Figure 4.9: Achievable weighted sum-rate  $a_1 = 2, a_2 = 1, \sigma_1^2 = 0.25, \sigma_2^2 = 1$  and  $\sigma^2 = 1$ .

rate ( $a_i = 1$  and  $X_i = 1 + \text{SNR}_i \forall i \in \{1, 2\}$ ) will be  $\text{SNR}_i = \gamma_{\max} \forall i \in \{1, 2\}$  which is equal to the optimal solution obtained in [18].

**Remark 2.** Using Theorem 4, the optimal solution for maximizing the common-rate ( $X_i = \text{SNR}_i \forall i \in \{1, 2\}$ ) for the rate region  $\Theta$  proposed in [18], can be obtained as  $\text{SNR}_i = \gamma_{\max} \forall i \in \{1, 2\}$  which is equal to the optimal solution obtained in [18].

# Chapter 5

## Conclusion & Future Works

In this thesis, we developed optimal solutions for weighted sum-rate and common-rate optimization problems subject to certain conditions on the feasible SNR region. Our solutions do not require the region to be convex. To verify our analyses, two examples of massive MIMO networks have been presented. Moreover, the results in [18] have been re-obtained using the presented theorems.

As the first example, a network of two MIMO terminals and a single-antenna relay has been considered. One of the terminals is a massive MIMO device. Subject to the total power constraint, we derived the exact closed-form optimal PA to maximize the sum rate using the presented framework in Chapter 3. The resulting sum rate is a function of instantaneous channel gains. Owing to the closed-form solution achieved and by exploiting the weak law of large numbers, we then derived the ergodic sum rates in closed-form. To provide a degree of generality, we used the Nakagami- $m$  fading model. We also derived a sub-optimal PA to maximize sum rate when the SNRs at both terminals must exceed target values. Both feasible and infeasible systems were simulated. Simulation results showed both the accuracy of the derived theoretical expressions and the efficiency of proposed PA strategies.

For the second example, a two-way relay network has been considered where the relay is equipped with a large-scale antenna array and the total transmit

power is constant. The common rate and weighted sum rate optimization problems have been investigated for this network. The closed-form optimal power allocations for these problems have been derived. Finally, simulation results verified the optimality of the obtained theoretical solutions. An advantage of closed-form optimal solutions is that they facilitate the investigation of performance measures such as ergodic sum-rate, outage and error rates. Thus, obtaining the closed-form expressions for outage and error rates of the considered networks may be of great interest.

Although the presented theorems provide the optimal closed-form solution for weighted sum rate and common rate optimization problems in many cases, some of the weighted sum rate and common rate problems remain unmanageable and hard to solve, e.g. when the effect of transmitter and receiver distortion is taken into account for a multi-user multi-cell network. Developing new theorems to obtain the closed-form solutions for the remaining cases is of great interest.

# Bibliography

- [1] ABI Research. The internet of things will drive wireless connected devices to 40.9 billion in 2020, 08 2014. URL <https://www.abiresearch.com/press/the-internet-of-things-will-drive-wireless-connect>.
- [2] G. J. Foschini, G. D. Golden, R. A. Valenzuela, and P. W. Wolniansky. Simplified processing for high spectral efficiency wireless communication employing multi-element arrays. *IEEE Journal on Selected Areas in Communications*, 17(11):1841–1852, Nov 1999. ISSN 0733-8716. doi: 10.1109/49.806815.
- [3] H. Q. Ngo, E. G. Larsson, and T. L. Marzetta. Energy and spectral efficiency of very large multiuser mimo systems. *IEEE Transactions on Communications*, 61(4):1436–1449, April 2013. ISSN 0090-6778. doi: 10.1109/TCOMM.2013.020413.110848.
- [4] J. N. Laneman, D. N. C. Tse, and G. W. Wornell. Cooperative diversity in wireless networks: Efficient protocols and outage behavior. *IEEE Transactions on Information Theory*, 50(12):3062–3080, Dec 2004. ISSN 0018-9448. doi: 10.1109/TIT.2004.838089.
- [5] D. Stamatelos and A. Ephremides. Spectral efficiency and optimal base placement for indoor wireless networks. *IEEE Journal on Selected Areas in Communications*, 14(4):651–661, May 1996. ISSN 0733-8716. doi: 10.1109/49.490416.

- [6] J. N. Laneman and G. W. Wornell. Distributed space-time-coded protocols for exploiting cooperative diversity in wireless networks. *IEEE Transactions on Information Theory*, 49(10):2415–2425, Oct 2003. ISSN 0018-9448. doi: 10.1109/TIT.2003.817829.
- [7] Y. Sankarasubramaniam, I. F. Akyildiz, and S. W. McLaughlin. Energy efficiency based packet size optimization in wireless sensor networks. In *Proceedings of the First IEEE International Workshop on Sensor Network Protocols and Applications, 2003.*, pages 1–8, 2003. doi: 10.1109/SNPA.2003.1203351.
- [8] Bruno Bougard, Francky Catthoor, Denis C. Daly, Anantha Chandrakasan, and Wim Dehaene. Energy efficiency of the iee 802.15.4 standard in dense wireless microsensor networks: Modeling and improvement perspectives. In *Proceedings of the Conference on Design, Automation and Test in Europe - Volume 1, DATE '05*, pages 196–201, Washington, DC, USA, 2005. IEEE Computer Society. ISBN 0-7695-2288-2. doi: 10.1109/DATE.2005.136. URL <http://dx.doi.org/10.1109/DATE.2005.136>.
- [9] P. Lettieri and M. B. Srivastava. Adaptive frame length control for improving wireless link throughput, range, and energy efficiency. In *INFOCOM '98. Seventeenth Annual Joint Conference of the IEEE Computer and Communications Societies. Proceedings. IEEE*, volume 2, pages 564–571 vol.2, Mar 1998. doi: 10.1109/INFCOM.1998.665076.
- [10] A. Jalali, R. Padovani, and R. Pankaj. Data throughput of cdma-hdr a high efficiency-high data rate personal communication wireless system. In *VTC2000-Spring. 2000 IEEE 51st Vehicular Technology Conference Proceedings (Cat. No.00CH37026)*, volume 3, pages 1854–1858 vol.3, 2000. doi: 10.1109/VETECS.2000.851593.
- [11] Maria Papadopouli and Henning Schulzrinne. Effects of power conserva-

- tion, wireless coverage and cooperation on data dissemination among mobile devices. In *Proceedings of the 2Nd ACM International Symposium on Mobile Ad Hoc Networking & Computing*, MobiHoc '01, pages 117–127, New York, NY, USA, 2001. ACM. ISBN 1-58113-428-2. doi: 10.1145/501431.501433. URL <http://doi.acm.org/10.1145/501431.501433>.
- [12] Mansoor Alicherry, Randeep Bhatia, and Li (Erran) Li. Joint channel assignment and routing for throughput optimization in multi-radio wireless mesh networks. In *Proceedings of the 11th Annual International Conference on Mobile Computing and Networking*, MobiCom '05, pages 58–72, New York, NY, USA, 2005. ACM. ISBN 1-59593-020-5. doi: 10.1145/1080829.1080836. URL <http://doi.acm.org/10.1145/1080829.1080836>.
- [13] Ekram Hossain, Dong In Kim, and Vijay K Bhargava. *Cooperative cellular wireless networks*. Cambridge University Press, 2011.
- [14] Christian Guthy, Wolfgang Utschick, Raphael Hunger, and Michael Joham. Efficient weighted sum rate maximization with linear precoding. *IEEE Transactions on Signal Processing*, 58(4):2284–2297, 2010.
- [15] Rui Zhang, Ying-Chang Liang, Chin Choy Chai, and Shuguang Cui. Optimal beamforming for two-way multi-antenna relay channel with analogue network coding. *IEEE Journal on Selected Areas in Communications*, 27(5), 2009.
- [16] Shama N Islam, Salman Durrani, and Parastoo Sadeghi. Optimum power allocation for sum rate improvement in af multi-way relay networks. In *Signal Processing and Communication Systems (ICSPCS), 2014 8th International Conference on*, pages 1–7. IEEE, 2014.
- [17] Zhi-Quan Luo and Shuzhong Zhang. Dynamic spectrum management:

- Complexity and duality. *IEEE Journal of Selected Topics in Signal Processing*, 2(1):57–73, 2008.
- [18] S. ShahbazPanahi and M. Dong. Achievable rate region under joint distributed beamforming and power allocation for two-way relay networks. *IEEE Trans. Wireless Commun.*, 11(11):4026–4037, November 2012. ISSN 1536-1276. doi: 10.1109/TWC.2012.092112.112072.
- [19] J Nicholas Laneman, David NC Tse, and Gregory W Wornell. Cooperative diversity in wireless networks: Efficient protocols and outage behavior. *IEEE Transactions on Information theory*, 50(12):3062–3080, 2004.
- [20] Anne Aaron, Rui Zhang, and Bernd Girod. Wyner-ziv coding of motion video. In *Signals, Systems and Computers, 2002. Conference Record of the Thirty-Sixth Asilomar Conference on*, volume 1, pages 240–244. IEEE, 2002.
- [21] Gerard J Foschini, Glenn D Golden, Reinaldo A Valenzuela, and Peter W Wolniansky. Simplified processing for high spectral efficiency wireless communication employing multi-element arrays. *IEEE Journal on Selected areas in communications*, 17(11):1841–1852, 1999.
- [22] L. Lu, G. Y. Li, A. L. Swindlehurst, A. Ashikhmin, and R. Zhang. An overview of massive mimo: Benefits and challenges. *IEEE Journal of Selected Topics in Signal Processing*, 8(5):742–758, Oct 2014. ISSN 1932-4553. doi: 10.1109/JSTSP.2014.2317671.
- [23] Jensen’s inequality. <https://brilliant.org/wiki/jensens-inequality>. Retrieved 17:45, May 24, 2017.
- [24] Proofs of am-gm. <https://artofproblemsolving.com/wiki>. Retrieved 17:58, May 24, 2017.

- [25] Raymond W. Yeung. *Information Theory and Network Coding*. Springer Publishing Company, Incorporated, 1 edition, 2008. ISBN 0387792333, 9780387792330.
- [26] T. K. Y. Lo. Maximum ratio transmission. In *1999 IEEE International Conference on Communications (Cat. No. 99CH36311)*, volume 2, pages 1310–1314 vol.2, 1999. doi: 10.1109/ICC.1999.765552.
- [27] S. Talwar, Y. Jing, and S. Shahbazpanahi. Joint relay selection and power allocation for two-way relay networks. *IEEE Signal Process. Lett.*, 18(2): 91–94, Feb 2011. ISSN 1070-9908. doi: 10.1109/LSP.2010.2096466.
- [28] L. Pang, Y. Zhang, J. Li, Y. Ma, and J. Wang. Power allocation and relay selection for two-way relaying systems by exploiting physical-layer network coding. *IEEE Trans. Veh. Technol.*, 63(6):2723–2730, July 2014. ISSN 0018-9545. doi: 10.1109/TVT.2013.2294650.
- [29] T. P. Do, J. S. Wang, I. Song, and Y. H. Kim. Joint relay selection and power allocation for two-way relaying with physical layer network coding. *IEEE Commun. Lett.*, 17(2):301–304, February 2013. ISSN 1089-7798. doi: 10.1109/LCOMM.2013.122013.122134.
- [30] M. S. Alouini and A. J. Goldsmith. Capacity of Rayleigh fading channels under different adaptive transmission and diversity-combining techniques. *IEEE Trans. Veh. Technol.*, 48(4):1165–1181, Jul 1999. ISSN 0018-9545. doi: 10.1109/25.775366.